Werk

Jahr: 1974
Kollektion: fid.geo
Signatur: 8 Z NAT 2148:40
Digitalisiert: Niedersächsische Staats- und Universitätsbibliothek Göttingen
Werk Id: PPN1015067948_0040
PURL: http://resolver.sub.uni-goettingen.de/purl?PPN1015067948_0040

LOG Id: LOG_0100
LOG Titel: The structure of the Ries crater from geoelectric depth soundings
LOG Typ: article

Übergeordnetes Werk

Werk Id: PPN1015067948
PURL: http://resolver.sub.uni-goettingen.de/purl?PPN1015067948
OPAC: http://opac.sub.uni-goettingen.de/DB=1/PPN?PPN=1015067948

Contact

Niedersächsische Staats- und Universitätsbibliothek Göttingen
Georg-August-Universität Göttingen
Platz der Göttinger Sieben 1
37073 Göttingen
Germany
Email: gdz@sub.uni-goettingen.de

J. Geophys. 40, 639–659, 1974

The Structure of the Ries Crater from Geoelectric Depth Soundings

K. Ernstson

Institut für Geophysik der Universität Kiel

Received March 4, 1974

Abstract. About 300 geoelectric depth soundings have been carried out in the Ries basin area in order to determine the crater structure. A map of lake sediment thickness is presented. In addition, cross sections of radial profiles have been plotted showing the complex structure of the inner rim with a distinct step-like transition to the central crater. The exact location of the central crater with its geometrical center is provided. Resistivity sections and profiles resulting from bilateral equatorial soundings in the central crater show a dish-like underground structure and, in particular, the existence of another ring wall with diameter of roughly 5 km. Resistivity profiles and upward continuation of the gravity field reveal that the central crater is asymmetric with the crater axis dipping to the east.

Key words: Meteorite Crater — Multi-Ring Basin — Crater Asymmetry — Suevite — Gravity and Geomagnetic Anomalies — Geoelectric Dipole Soundings.

1. Introduction

The Ries basin is a prominent ring structure of some 25 km in diameter, located in southern Germany about 120 km northwest of Munich. Controversy has been in the past whether the Ries basin originated from a volcanic explosion or a giant meteorite impact, but now there is no doubt that the Ries crater is of impact origin. The impact occured about 15 million years ago (Gentner and Wagner, 1969) and this means the Ries crater is a very young structure. Moreover it is very well preserved owing to the filling-in of lake deposits after the impact. But on the other hand, these lake sediments hinder direct geologic and topographic work on the original crater. Up to now deep bore holes are lacking and that is why geophysical investigations have hitherto given most information about the deeper crater structure. The early refraction work (Reich and Horrix, 1955) has given a rough view of the crater down to a depth of a few hundred meters, showing the existence of an inner crater which is surrounded by the so-called inner or crystalline rim. Gravity methods have established a strong negative anomaly (Jung *et al.*, 1969). According to the volcanic theory, the negative anomalies of the total intensity of the geomagnetic field were first referred to basaltic intrusions (Reich and Horrix, 1955). A new geomagnetic and seismic survey (Pohl and Angenheister, 1969; Angenheister and Pohl,

1969), however, has revealed a suevite layer of reverse magnetization below the lake sediments to be the cause of negative magnetic anomalies within the inner rim. Measurements of seismic velocity have suggested that the layer below the suevite may consist of fractured crystalline rocks. Their P-velocity down to a depth of at least 2,5 km is smaller than the velocity of the undisturbed basement outside the crater (Angenheister and Pohl, 1969).

A comprehensive presentation of geological, mineralogical, and geophysical investigations on Ries basin is to be found in a monograph (Bayer. Geologisches Landesamt, 1969). In addition, a review paper was published by Dennis (1971).

The present article summarizes results of a detailed geoelectric survey including a great deal of depth soundings which have been carried out in the last years. This work was primarily done in order to get an idea of the fine crater structure, first of all of the shape of the inner rim. But the intention was also to complement seismic investigations as well as gravity and geomagnetic survey which are ambiguous without additional information.

2. Geoelectric Measurements

The geoelectric measurements in the Ries basin include about 300 depth soundings lying on 15 radial and 3 diametrical profiles (Fig. 1). The mean distance between soundings on the radial profiles is about 400 m, and 1 km on the diametrical profiles, respectively. Quite a few soundings have been carried out between these profiles and outside the morphological rim, too. For the location of all depth soundings within the morphological rim see Fig. 5. Both, Schlumberger and dipole electrode configurations have been used for measuring ground resistivity. Soundings on the diametrical profiles within the central crater have been made by bilateral equatorial arrays only. In the equatorial array, the two dipoles are placed parallel to one another, each being centered on the equatorial axis of the other. A bilateral sounding is made by moving two measuring dipoles to opposite directions, the current dipole being fixed. Thus, one gets two sounding curves which provide a high resolving power over dipping beds.

An unpublished collection of all sounding curves is available from the *Institut für Geophysik der Universität Kiel.*

3. Resistivities of Rocks from the Ries Crater Area

The Upper Miocene lake sediments of the Ries basin usually are covered with Pleistocene deposits such as loess, loess clay, or fluviatile sands and gravels. Gathered from soundings at bore holes, the resistivities are:

loess and loess clay	10— 20 Ωm
sands and gravels	150—400 Ωm.

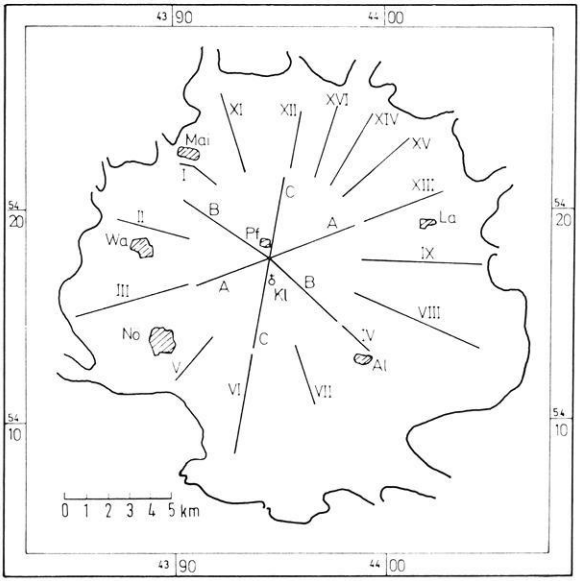

Fig. 1. Location map of geoelectric profiles. Solid line: Morphological boundary of the Ries plane (*Al* Alerheim, *Dei* Deiningen, *Kl* Klosterzimmern, *La* Laub, *Mai* Maihingen, *Nö* Nördlingen, *Oe* Oettingen, *Pf* Pfäfflingen, *Wa* Wallerstein; also valid for the following Figures)

The Upper Miocene lake sediments consist of clay and marl which show a characteristic resistivity distribution. As a rule resistivities decrease with increasing depth implying a rough classification into an upper layer with resistivities of 8—15 Ωm, and a lower layer with typical values of 3—5 Ωm. Deviations from the rule are possible.

As underlying bed of the lake sediments *Bunte Trümmermassen*, *Bunte Breccie*, *Kristallinbreccie*, or suevite are considered. These rocks are also present at some places without younger covering which, in contrast with the lake deposits, makes them accessible to direct soundings. Table 1 gives results of resistivity measurements on exposed rock.

Numerous resistivity measurements have been carried out at suevite deposits in quarries outside the crater rim. The results are given in Table 2.

The resistivity of the suevite seems to be really small. The good conductivity, however, can be explained by a high porosity and the contents of clay minerals. Thus, porosities up to 37% have been found in the bore holes Deiningen and Wörnitzostheim (Förstner, 1967).

Concerning clay minerals, montmorillonite is predominant, filling vesicles and fissures of glasses and matrix (Engelhardt *et al.*, 1969).

Table 1. Resistivities of Exposed Rock from the Ries Crater Area

Rock	Location	Resistivity, Ωm
Crystalline rock (granite)	Wennenberg	150–300
Crystalline rock (granite)	Langenmühle	70
Crystalline Breccia	Meyers Keller Nördlingen	20–60
Bunte Breccie	Suevite quarry Otting	20
Bunte Breccie	Suevite quarry Aumühle	20–30
Opalinus shales (Dogger)	single klippen near Fremdingen	14–15
Malmian limestone	Metzlesberg	40–80
Keuper sandstone (Burgsandstein)	north of Fremdingen	40–100

Table 2. Resistivities of suevite from quarries

Location	Resistivity, Ωm
Polsingen	50–80
Aumühle	12–30
Zipplingen	10–13
Aufhausen	30–45
Amerdingen	12–20
Bollstadt	20–50
Otting	12–35
Spielberg	55

4. *Typical Sounding Curves*

Fig. 2 shows the sounding curves ES 73 and ES 52 that have been measured near Nördlingen. ES 73 (Gauß-Krüger-coordinates: R = 4390450, H = 5411925) is located in the zone of the inner rim and ES 52 (R = 3609600, H = 5415725) at the boundary of the central crater. In addition, Fig. 2 gives a possible interpretation (logarithmic scale) for an assumed section: humus — loess or loess clay — sand or gravel — Upper Miocene clay — *Riestrümmermassen*. At ES 73 the base of the lake sediments in about 50 m beneath the surface, and at ES 52 about 200 m.

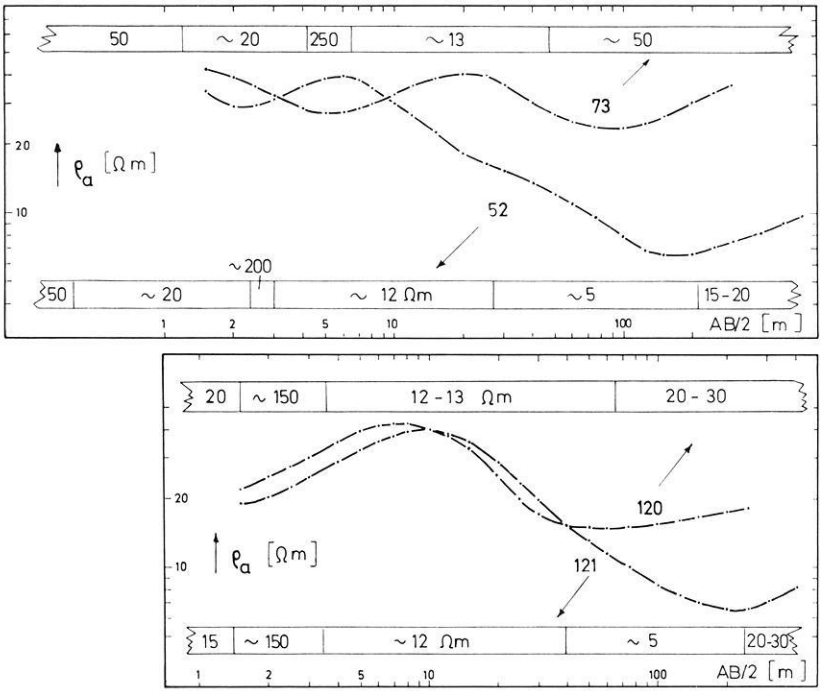

Fig. 2, 3. Typical sounding curves from the Ries basin with the interpreted layers and their resistivities (in Ωm). For the lithologic character of the layers see text

ES 120 (R = 4399600, H = 5415475) and ES 121 (R = 4399225, H = 5415725) (Fig. 3) show a characteristic transition from the inner rim to the central crater near Fessenheim. The lower boundary of the lake sediments goes down about 170 m along a distance of about 500 m, implying a dip of 20°.

All the sounding curves have been interpreted by the auxiliary point method, using 3- and 4-layer master curves. It must be mentioned that because of often unknown true resistivities the depths of strata are approximate only and sometimes serious errors may occur in the interpretation of the measured sounding curves.

The sounding curves in the central crater are all quite similar. The lake sediments are subdivided into an upper layer with a thickness of about 20—40 m (resistivity 8—10 Ωm) and a lower layer which is more than 200 m thick (resistivity 3—5 Ωm). The right-hand portions of the curves have always been measured by bilateral equatorial soundings. As a rule, the plus and minus curves show a noticeable difference (Fig. 4). This will be used below to describe the deeper crater structure.

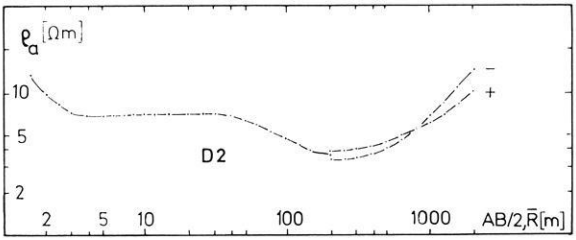

Fig. 4. Sounding curve from the central crater. The left-hand portion has been measured by the Schlumberger configuration, the right-hand portion by a bilateral equatorial dipole sounding. R̄, commonly called the actual spacing, is the distance between one current electrode and the center of the measuring dipole

5. Thickness of the Tertiary Lake Sediments

The interpretation of all sounding curves has led to a plot of lines of equal lake sediment thickness (Fig. 5). This plot can be taken as the topography of the crater before sedimentation. Disregarding subsequent erosion and tectonics this will mean the topography shortly after the impact. Because of unknown resistivities the lower boundary of the lake sediments in the central crater could not be established definitely by geoelectric depth soundings, but according to seismic measurements (Reich and Horrix, 1955; Angenheister and Pohl, 1969) this boundary is like a flat dish with its deepest point about 350 m below the surface.

Fig. 5 gives some idea of the complex structure of the outer crater zone between the inner rim and the morphological rim. On the whole, the northern part of this zone differs from the southern part by a greater average thickness of the lake sediments. Obviously this means that there less ejecta have been deposited. Thus, the often discussed asymmetric distribution of the ejecta seems to be present in the crater itself. The geological map (Bayer. Geologisches Landesamt, 1969) illustrates the predominant existence of ejecta in the south and southeast of the Ries crater. Hüttner (1969) estimates this uneven distribution to be the result of a different post-Ries erosion on the Alb plateau and in the Alb foreland. This interpretation is not applicable to the crater itself. Here the Alb scarp, crossing the Ries in an east-west direction, may have been of some importance so that in the south of the Ries the entire Malm strata have been affected by the burst while in the north it had only result on the Alb foreland (Kranz, 1949).

As mentioned before the base of the lake sediments could not be found out definitely by geoelectric depth soundings. There is, however, some possibility to make statements on relative changes in the thickness of the lake sediment layer. The most important part of the sounding curves in the cen-

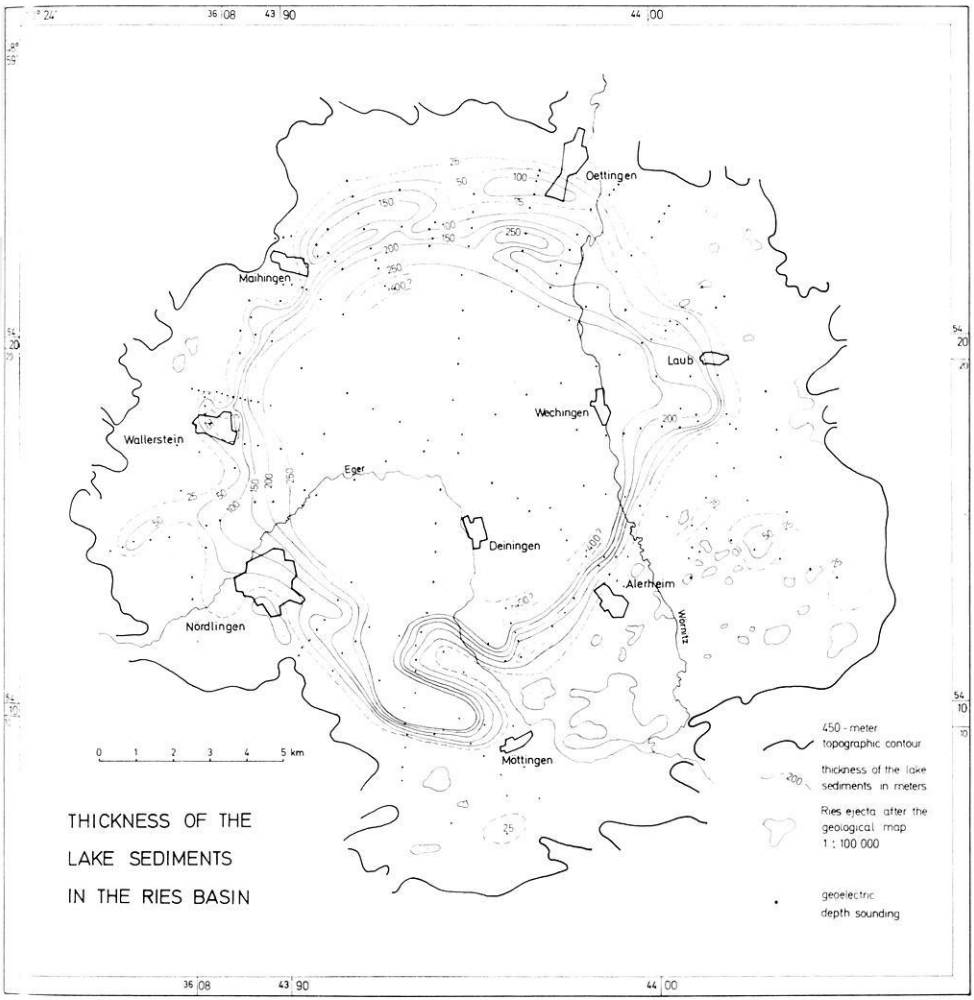

Fig. 5. Thickness of the Tertiary lake sediments in the Ries basin from geoelectric depth soundings. In the central basin lines have been omitted because of doubtful interpretation of the sounding curves

tral crater is of minimum or H type (m_1 = thickness of the upper lake sediment layer with resistivity ϱ_1, m_2 = thickness of the lower lake sediment layer (ϱ_2), m_3 = thickness of the suevite or fractured crystalline rock (ϱ_3); see Fig. 4). Assuming m_1, ϱ_2/ϱ_1, and ϱ_3/ϱ_2 to be constant the minimum apparent resistivity $\varrho_{a,\,min}$ is a function of the thickness m_2 so that a smaller $\varrho_{a,\,min}$ corresponds to a greater thickness m_2. For the central crater in Fig. 6

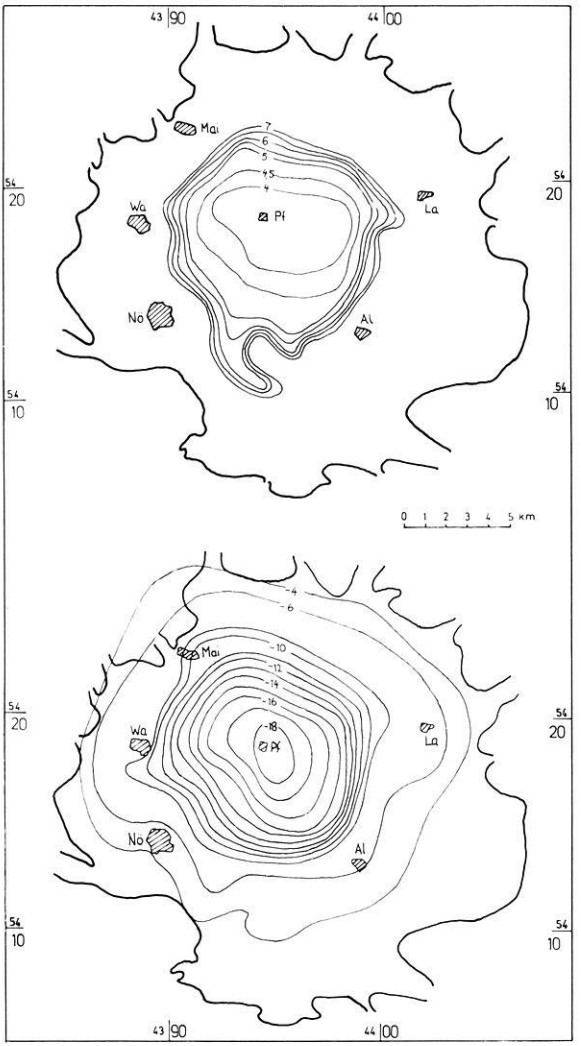

Fig. 6. Comparison of geoelectric and gravity measurements. Top: Lines of equal minimum apparent resistivity (isoohms). Values are Ohm·meters. Bottom: Gravity residual field 3 (after Kahle 1968, simplified). Values are mgals

lines of equal minimum apparent resistivity are plotted. They may be called — not quite correctly — isoohms. Below, the gravity residual field 3 (Kahle, 1969) is shown. Comparing the plot of isoohms with that of isogals there is quite a similarity. This correlation seems to be plausible as the gravity anomaly primarily shows the near-surface mass distribution which

is the mass distribution of the lake sediments in the Ries crater. Thus the isoohms may be understood as lines of equal thickness of the lake sediments without saying anything about the true thickness. A restriction is yet to be made as $\varrho_{a,\,min}$ depends on the resistivity of the underlying bed, too. There is often a correlation between the density of rock and its resistivity so that a higher density correlates with a higher resistivity. Consequently, the approximately identical pattern of the isoohms and the isogals may be caused by the rock below the lake sediments. Both effects cannot be distinguished.

There is a problem in interpreting gravity anomalies in the Ries concerning the construction of a true regional field. These difficulties have been pointed out by Jung and Schaaf (1967), and so different interpretations by these authors as well as by Kahle (1968) result in eight different regional fields. They correspond to eight residual fields and just as many different mass deficiencies (20,000—105,000 megatons). From these eight residual fields a special one can be selected which shows the best fit to the plot of isoohms. Hence, the gravity residual field 3 (Fig. 6) most probably is the best approximation to the true Ries gravity anomaly.

6. Radial Profiles — Cross Sections of the Inner Rim

The small scale of the map in Fig. 5 has necessitated some simplifications. More detailed informations on the structure of the inner rim may be obtained from cross sections of the radial profiles. Cross sections of all 15 radial profiles are given in Ernstson (1974). Some typical ones showing the lower boundary of the lake deposits (i.e. the surface of the inner rim) will be described below (Figs. 7—11). The depths of the horizons are always related to the surface which, for simplification, has been taken to be even. This seems to be justified as the very flat topography of the Ries plane only causes a slight distortion of the true boundary layers. The strongly exaggerated cross sections may not deceive about the fact that, as a rule, there are only flattened structures.

Fig. 7 shows the surface of the inner rim along profile II running from the west to the east near Wallerstein. As most other profiles will show, too, the steplike transition to the central crater is a characteristic feature of the inner rim. The dashed line indicates a horizon within the lake sediments which separates an upper layer with resistivities of 9—14 Ω m from a lower thick layer with a resistivity of about 5 Ω m. The steep dip (about 40°) of the lake sediment base between ES 8 and ES 31 marks the boundary of the central crater.

Fig. 8 shows the cross section of the noteworthy tonguelike depression in the south of the crater being connected with the central basin (see also Fig. 5). The maximum thickness of the lake sediments is about 300 m.

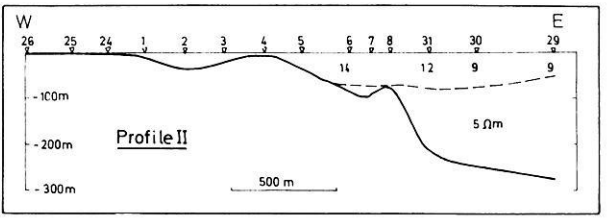

Fig. 7. Cross section of the inner rim near Wallerstein. Full line: Lower boundary of the lake sediments Dashed line: Horizon within the lake sediments

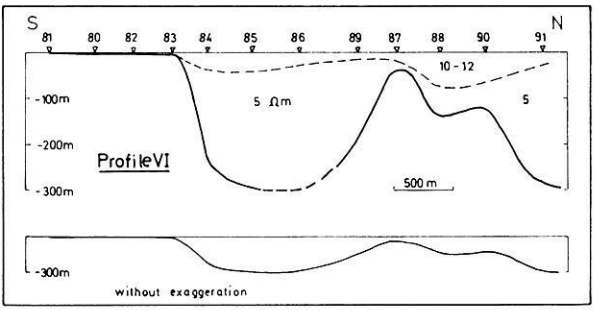

Fig. 8. Cross section of the tonguelike depression and the inner rim in the south of the crater

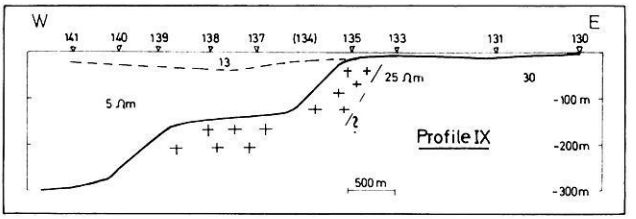

Fig. 9. Transition from the inner rim to the central crater in the east of the Ries basin. + + +: crystalline (?) rock

This is in agreement with depth estimations derived from seismic refraction measurements (Reich and Horrix, 1955). Reich thought this depression to be an external pit crater, but with regard to geoelectric measurements there is no evidence for such an interpretation.

Profile IX (Fig. 9) is located to the east of the crater and shows a steplike transition from the inner rim to the central crater. Somewhat higher resistivities (>100 Ω m) of the rock below the lake sediments are probably due to minor fractured crystalline klippen which form the inner rim.

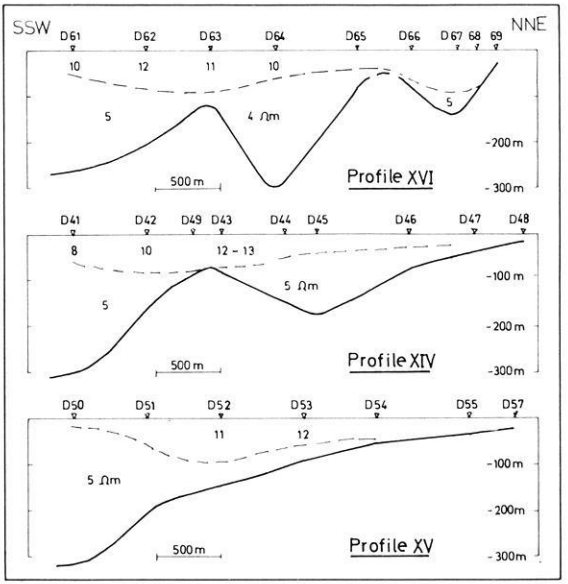

Fig. 10. Cross section of the inner rim in the north of the crater

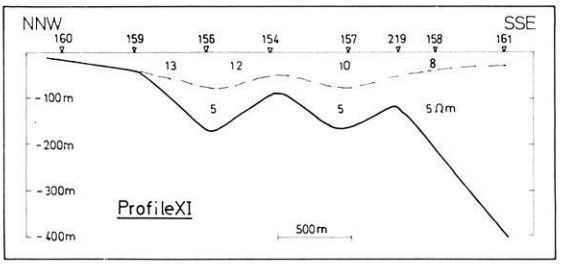

Fig. 11. Cross section of the inner rim near Maihingen

Up to now the north of the Ries crater had a sort of exceptional position because of a gap of the inner rim that was required by seismic refraction work (Reich and Horrix, 1955) leading to the concept of the "horseshoe-like" ring wall and, later on, to the assumption that the impacting body came from the north. In a previous short paper (Ernstson, 1972) a preliminary qualitative interpretation of bilateral equatorial dipole soundings has shown that the idea of a horseshoe-like inner ring no longer is valid. Meanwhile, additional investigations have been carried out including a quantitative interpretation of sounding curves that leads to cross sections shown in Fig. 10.

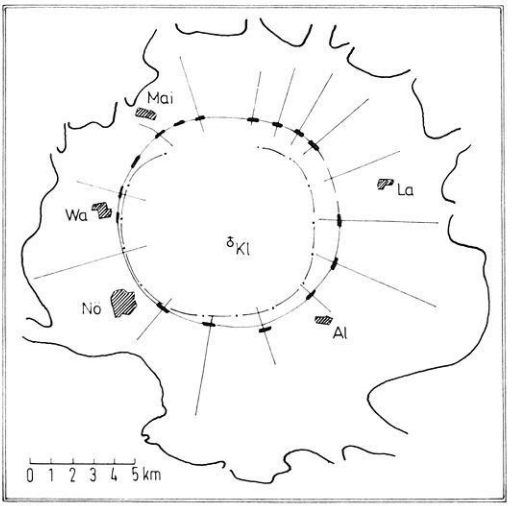

Fig. 12. Boundary of the central crater from geoelectric depth soundings (solid line) and gravity interpretation (·—·—· ; after Kahle (1968))

Profile XI (Fig. 11) running from NNW to SSE near Maihingen is characterized by a distinct steplike structure of the inner rim. The boundary layer within the lake sediments (dashed line) is nearly parallel to the surface of the inner rim (quite similar to profile VI, Fig. 8), and this is thought to be an indication for a post-Ries sinking of the inner rim.

7. Boundary of the Central Crater

As has been seen from the cross sections of the radial profiles the boundary of the central crater is indicated by a relatively steep dip of the lake sediment base. In Fig. 12 the transition from the inner rim to the central crater has been marked by a heavy dash. These marks lie nearly on a circle providing the diameter of the central crater to be about 10,5 km and its center being located 1 km north of Klosterzimmern. In addition, Fig. 12 shows the boundary of the central crater resulting from interpretations of the gravity residual field (Kahle, 1968).

8. Dipole Soundings in the Central Crater-Innermost Ring Wall

Since at present true resistivities of rock beneath the lake sediments are unknown the following statements primarily deal with a qualitative interpretation of bilateral equatorial soundings with considerable depth penetration (2000 m maximum dipole separation) in the central crater. Re-

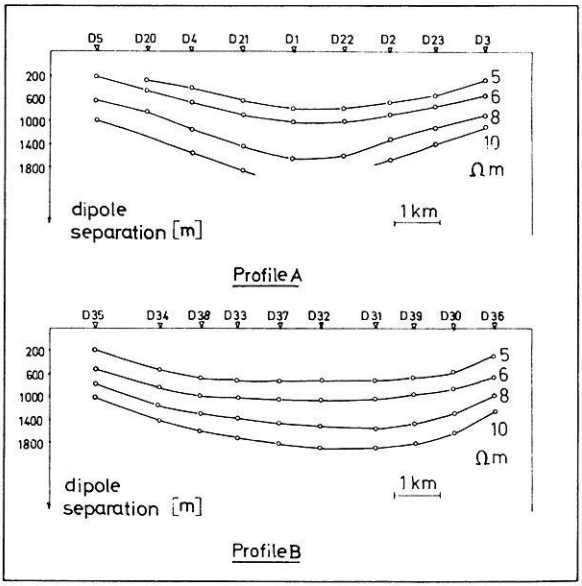

Fig. 13. Apparent resistivity sections from the central crater

sistivity cross sections have been constructed for the diametrical profiles A and B with the average values of plus and minus resistivity plotted at the array centers (Fig. 13). Thus, one gets an idea of the dish-like underground structure as is expected for a meteorite crater.

Seismic studies on a profile near Wallerstein have provided evidence that below the lake sediments there is a refraction marker showing also some weak reflections (Angenheister and Pohl, 1969). This horizon is thought to be the base of a suevite layer. In particular, an upbowing of the horizon must be mentioned which, because of the correlation with magnetic anomalies, leads to the concept that generally a strong negative anomaly indicates a considerable suevite thickness and, vice versa, a small negative or even positive anomaly is due to a thin or even lacking suevite layer. In order to confirm this concept in principle, results of the geoelectric depth soundings have been compared with measurements of the total magnetic field intensity. This is illustrated in Fig. 14 showing the anomalies of ΔT plotted along the diametrical geoelectric profiles. (ΔT is the difference between the measured total intensity T and a regional field.) All magnetic data have been taken from an isanomalic contour map (Pohl and Angenheister, 1969). To construct the geoelectric profiles of Fig. 14 it has been assumed that the right-hand portion of the sounding curves is of A type (see Fig. 4): $\varrho_{ls} < \varrho_{su} < \varrho_{fc} \cdot \varrho_{ls}$, ϱ_{su}, ϱ_{fc} are the resistivities of the lake

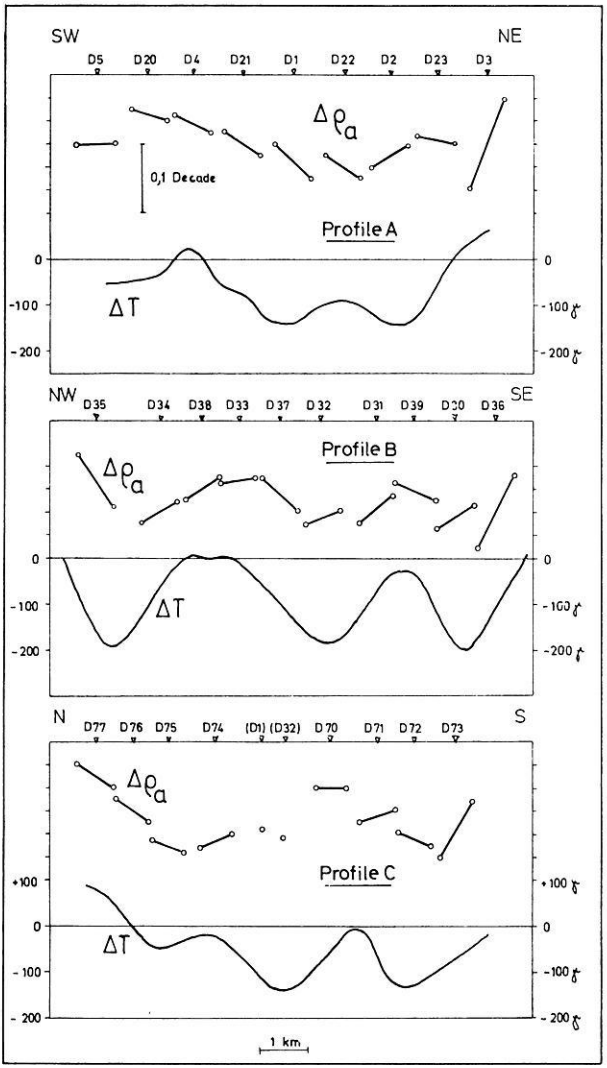

Fig. 14. Comparison of geoelectrics ($\Delta\varrho_a$) and geomagnetics (ΔT) concerning the suevite thickness

sediments, suevite, and fractured crystalline rock. As for the A type, the first slope of the curve is a measure of the second layer thickness, the resistivity of the third layer being constant. For the sounding curves in the central crater that means: The steeper the slope the thinner the suevite layer should be. From this the construction of the geoelectric profiles results, dispensing with assumptions on true resistivities but using direct

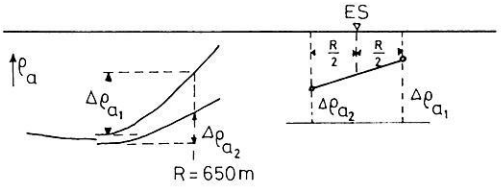

Fig. 15. On the construction of the geoelectric profiles from Fig. 14

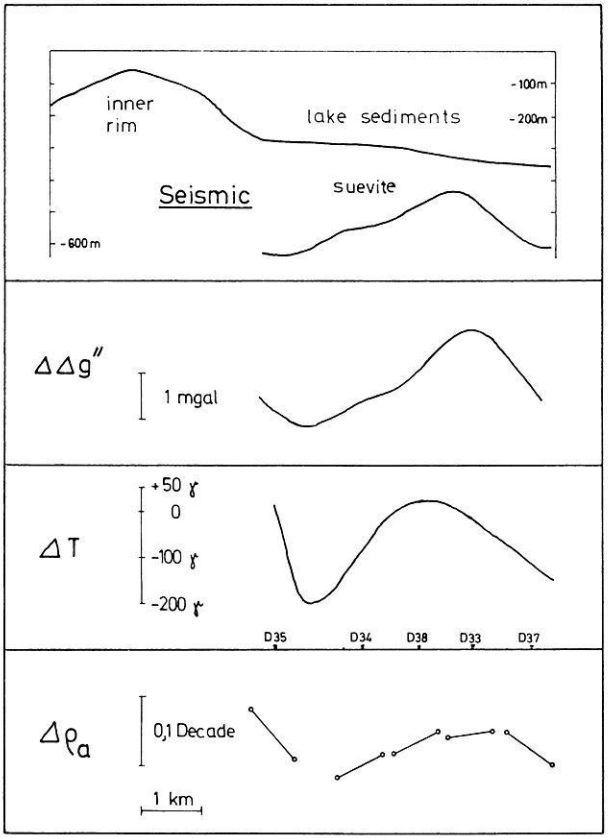

Fig. 16. Seismic, gravity, geomagnetic, and geoelectric profiles across the upbowing below the lake sediments east of Wallerstein (Seismic and magnetic profiles after Angenheister and Pohl 1969). $\Delta\Delta g''$ is the difference between Bouguer anomaly and a gradient concerning the radial decrease of gravity due to the nearly concentric negative anomaly. The geoelectric profile is part of the profile B in Fig. 14

measurements only. For both, plus and minus curves the distance $\Delta\varrho_a$ between the apparent resistivity, referred to a 650 m dipole spacing, and the minimum apparent resistivity has been evaluated using the middle between current and measuring dipole as reference point (Fig. 15). The N—S profile C includes the soundings ES D1 and ES D32 being located some 300 m east of the profile and their average $\Delta\varrho_a$ referred to the array center. Although this construction method is based on rather simple assumptions the good correlation between magnetics and geoelectrics is obvious and demonstrates the validity of the stated concept.

In addition, a new special gravity survey has been carried out along a profile nearly parallel to the seismic reflection profile east of Wallerstein, showing clearly an upbowing composed of rocks with a higher density than the neighbouring suevite (Fig. 16).

Returning to Fig. 14, it is evident that the distribution of magnetic anomalies (and therefore suevite) is not random. Strong negative anomalies can be found in a marginal zone of the central crater, another one is located nearly at the center of the crater. Between these, upbowings exist which, summarizing results of geophysical measurements, consist of material of higher density, resistivity, and seismic P velocity but lacking negative magnetization. As has been pointed out earlier by Angenheister and Pohl (1969) this material is thought to be less fractured crystalline rock with an induced positive magnetization (Pohl, 1971).

In Fig. 17 the crests of these structures from geoelectric and gravity measurements have been marked. According to Will (1970) there is also some evidence for an upward bowing on the seismic refraction profile 10. Fig. 17 gives an idea of the elliptical shape of the ring-like structure with a diameter of roughly 5 km. This structure will be called the innermost ring wall. It cannot be decided whether the upbowings are continuous or peak-like. To answer the question of the formation of this ring we remember the reverse convergent flow of material due to the release of shock compression (David, 1969), and it is suggested that the innermost ring wall may have been the beginning of a central uplift formation.

A somewhat surprising result was obtained by Johnson and Vand (1967) applying a data smoothing technique by Fourier analysis to topographic contours of Ries area. Outside the main rim (diameter 24 km) the authors established the existence of two extra rims with 34 and 45 km in diameter. Including the inner (or crystalline) rim and the innermost ring wall a system of five rings for the Ries crater is obtained, similar to the multi-ring systems of large lunar craters. A characteristic feature of these ring systems is the ratio of successive ring diameters to be usually about $\sqrt{2}$ or 2 (Hartmann and Wood, 1971). These multi-ring structures are supposed to be the result of frozen shock waves or some interference connected with the mechanism of shock wave propagation after the impact.

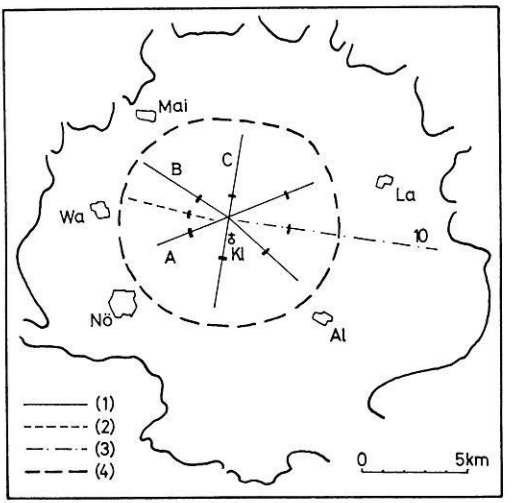

Fig. 17. Innermost ring wall. Crests of upbowings below the lake sediments:
(1) on geoelectric profiles
(2) on gravity profile
(3) on seismic profile (after Will 1970)
(4) boundary of the central crater

Another explanation is Baldwin's tsunami theory (1972). Referring to the Ries crater the following series of diameters is obtained

45 34 24 11,5 5 km

where 11,5 km for the diameter of the inner rim is a mean value which has been found by averaging the distances between the rim crest on the geoelectric radial profiles and the central crater midpoint. The ratios of successive ring diameters are

1,3 1,4 2,1 2,3

and, hence, are in good agreement with the above spacing law. However, it must be mentioned that the "true" center of the outer rings as calculated by Fourier analysis is about 2,5 km off the center of the Ries crater established by geoelectric measurements.

9. Asymmetric Deeper Structure

Fig. 18 shows two resistivity profiles which have been constructed for the geoelectric profiles A and B. For a dipole spacing of 1600 m apparent resistivity values have been taken from plus and minus sounding curves. The reference points for the two values of apparent resistivity (midpoints of lines connecting the center of both, current and measuring dipole) are joined by a straight line (the resistivity line). It should be noted

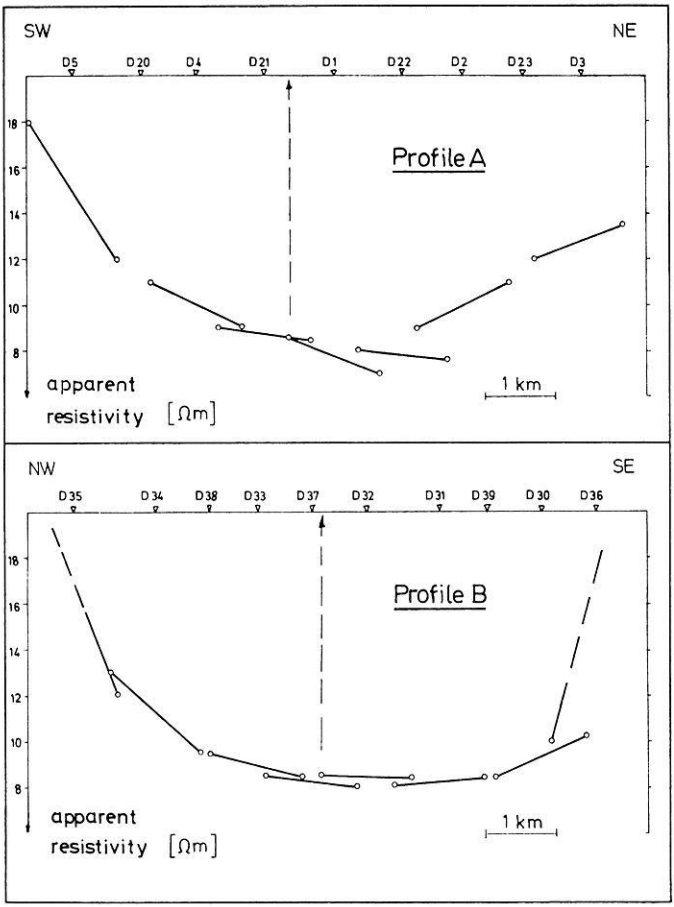

Fig. 18. Apparent resistivity profiles for a dipole separation of 1600 m. Arrows indicate the center of the inner crater rim

that this construction differs from that of Fig. 14. The resistivity lines in Fig. 18 nearly become a continuous curve pointing out the dish-like structure of the crater. The steep rise of the resistivity lines of the soundings ES D35 and ES D36 is caused by the fact that for large spacings the measuring dipoles already move above the inner rim of higher resistivity. It cannot be decided whether the resistivity profiles indicate a defined horizon of appreciable resistivity contrast or a transition zone, say a change from intensely fractured crystalline rocks to less fragmented basement.

In Fig. 18 the asymmetry of the resistivity profiles, related to the drawn-in arrows, is conspicuous. These arrows mark the intersection point of the profiles A and B which is identical to the center of the central crater rim

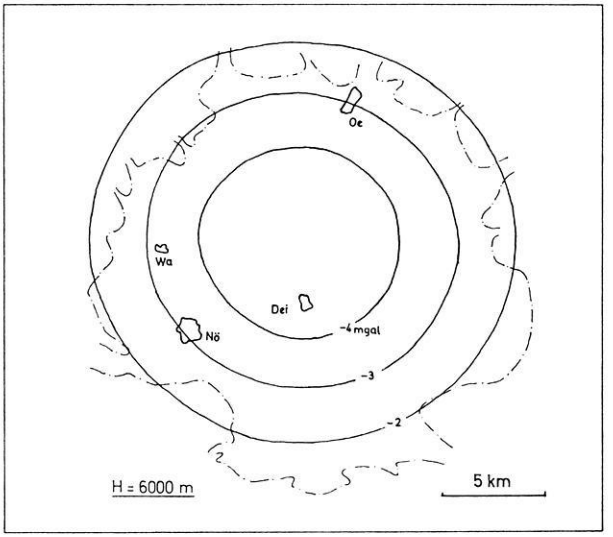

Fig. 19. Upward continuation of the gravity residual field. Continuation height: 6000 m above reference plane

as has been established by geoelectric measurements (see 7.). This means: The center of the deeper crater structure does not coincide with the center of the inner crater rim but is shifted to the east. The difference is about 1,5 km on profile A, and 1 km on profile B.

Considering the upward continuation of the gravity residual field there is some more evidence for an asymmetry of the crater. Fig. 19 shows the gravity anomaly that has been computed for the residual field 3 (see Fig. 6) for a continuation height $H = 6000$ m above reference plane. As can seen from Fig. 19 the strongly smoothed Ries anomaly is described by nearly concentric isogals of elliptical shape with the semimajor axis striking westeast.

The observed asymmetry may be considered to be the result of an oblique impact from direction west or east, respectively, confirming the theory that the Bohemian tectites (moldavites) have been ejected from the Ries crater (Vand, 1965; David, 1966), However, it must be mentioned that an oblique impact is not the only explanation for the observed asymmetry. The influence of the pre-Ries topography and the pre-Ries relief of the basement surface on the formation of the crater are also discussed (Ernstson, 1974).

The geoelectric measurements can by no means give any argument for an impact direction from north-northwest as has been established by Illies (1969). Illies' theory is based, among other things, on the well-known asymmetric distribution of the Ries ejecta and, especially, on results of previous geophysical measurements. Using the shape and the location of

the Bouguer gravity anomalies, for example, Illies deduces a flight direction (NNW to SSE), an angle of impact trajectory (13°), and an impact location (NW of Dürrenzimmern). As has been pointed out by Kahle (1968, 1969) the evaluation of the gravity residual field (describing the true anomaly) strongly depends on the arbitrariness in constructing the pre-Ries regional gravity field. Therefore the Bouguer anomaly seems not to be suitable for conclusions concerning impact features.

The geoelectric measurements can give a somewhat more founded argument for the impact location. According to 7., the center of the inner crater rims is located 1 km north of Klosterzimmern. This point or — taking into account the dipping crater axis — a point somewhat more in the east is thought to be the impact position, that means the point from which shock wave has started. This is in good agreement with results of mineralogic investigations: Graup (private communication), who analyzed shock effects on biotite of crystalline klippen, found that trajectories of shock wave propagation intersect in a point positioned 1 km northeast of Klosterzimmern. But yet there is no explanation for the discrepancy between the centers of the crater, one established by geoelectric and mineralogic research, the other found by Fourier analysis.

Acknowledgements. My thanks go to Prof. Dr. R. Meißner for his advice and support, to all colleagues of the Institut für Geophysik der Universität Kiel, who have helped with geoelectric field work, to Dr. J. Pohl for discussion and critical comments, to K.-D. Schaa, who has computed the upward continuation of the gravity residual field, to J. Zschau for reading the manuscript, to the Deutsche Forschungsgemeinschaft for financial support of this study.

References

Angenheister, G., Pohl, J.: Anomalien des Erdmagnetfeldes und Magnetisierung der Gesteine im Nördlinger Ries. Geol. Bavarica *61*, 327–336, 1969

Baldwin, R. B.: The tsunami model of the origin of ring structures concentric with large lunar craters. Phys. Earth Planet. Interiors *6*, 327–339, 1972

Bayer. Geologisches Landesamt, ed.: Das Ries. Geologie, Geophysik und Genese eines Kraters. Geol. Bavarica *61*, 478p., 1969

David, E.: Großmeteoriteneinschläge und Tektite. Z. Geophys. *32*, 539–550, 1966

David, E.: Das Riesereignis als physikalischer Vorgang. Geol. Bavarica *61*, 350–378, 1969

Dennis, J. G.: Ries structure, Southern Germany, A Review. J. Geophys. Res. *76*, 5394–5406, 1971

Engelhardt, W. v., Stöffler, D., Schneider, W.: Petrologische Untersuchungen im Ries. Geol. Bavarica *61*, 229–295, 1969

Ernstson, K.: Geoelektrische Messungen im Nördlinger Ries. Zum Verlauf des inneren Walls. Z. Geophys. *38*, 949–951, 1972

Ernstson, K.: Zum Aufbau des Ries-Kraters. Geoelektrische Untersuchungen und ihre Interpretation. Dissertation, Kiel, 1974

Förstner, U.: Petrographische Untersuchungen des Suevit aus den Bohrungen Deiningen und Wörnitzostheim im Ries von Nördlingen. Contr. Mineral. and Petrol. *15*, 281–308, 1967

Gentner, W., Wagner, G. A.: Altersbestimmungen an Riesgläsern und Moldaviten. Geol. Bavarica *61*, 296–303, 1969

Hartmann, W. K., Wood, C. A.: Moon: Origin and Evolution of Multi-Ring Basins. The Moon, Vol. 3 No. 1, 1971

Hüttner, R.: Bunte Trümmermassen und Suevit. Geol. Bavarica *61*, 142–200, 1969

Illies, H.: Nördlinger Ries, Steinheimer Becken, Pfahldorfer Becken und die Moldavite: strukturelle und dynamische Zusammenhänge einer Impact-Gruppe. Oberrhein. geol. Abh. *18*, 1–31, 1969

Johnson, G. G., Vand, V.: Application of a Fourier Data Smoothing Technique to the Meteoritic Crater Ries Kessel. J. Geophys. Res. *72*, 1741–1750, 1967

Jung, K., Schaaf, H.: Gravimetermessungen im Nördlinger Ries und seiner Umgebung, Abschätzung der gesamten Defizitmasse. Z. Geophys. *33*, 319–345, 1967

Jung, K., Schaaf, H., Kahle, H.-G.: Ergebnisse gravimetrischer Messungen im Ries. Geol. Bavarica *61*, 337–342, 1969

Kahle, H.-G.: Gravimetrische Untersuchungen über die Massenänderungen beim Riesereignis. Diplomarbeit, Kiel, 1968

Kahle, H.-G.: Abschätzung der Störungsmasse im Nördlinger Ries. Z. Geophys. *35*, 317–345, 1969

Kranz, W.: Zum Problem des Rieses und des Steinheimer Beckens. In: Das Problem des Rieses. Ed.: Oberrh. Geol. Ver., Nördlingen, 1926

Kranz, W.: Achte Fortsetzung der Beiträge zum Nördlinger Riesproblem. N. Jb. Miner. etc., Mh., 1949, B, 154–173, 1949

Pohl, J.: Magnetisierung der Gesteine und Interpretation der Anomalien des Erdmagnetfeldes im Ries-Krater. Dissertation, München, 1971

Pohl, J., Angenheister, G.: Anomalien des Erdmagnetfeldes und Magnetisierung der Gesteine im Nördlinger Ries. Geol. Bavarica *61*, 327–336, 1969

Reich, H., Horrix, W.: Geophysikalische Untersuchungen im Ries und Vorries und deren geologische Deutung. Beih. Geol. Jb. *19*, 119 p., 1955

Vand, V.: Terrestrial Meteoritic Craters and the Origin of Tectites. Advan. Geophys. *11*, 1–114, 1965

Will, M.: Seismik Ries 1968, II. Auswertung der Refraktionsmessungen. Diplomarbeit, München, 1970

Dr. K. Ernstson
Institut für Geophysik
der Universität
D-2300 Kiel
Neue Universität, Haus B 2
Federal Republic of Germany

Note Added in Proof. Resistivity well logging measurements carried out in the 1200 m drillhole Nördlingen, 1973 in the Ries crater have now provided true rock resistivities. Furthermore, resistivity measurements of cores have shown that the lake sediments are to a considerable extent anisotropic. So it will be possible and necessary to reinterpret the measured sounding curves in order to get exacter depths of strata.

Reference

Ernstson, K.: Untersuchungen zur elektrischen Leitfähigkeit in der Forschungsbohrung Nördlingen 1973. Geol. Bavarica *72*, 1974